Hindawi
Journal of Nanomaterials
Volume 2019, Article ID 2730317, 10 pages
https://doi.org/10.1155/2019/2730317

Research Article

A Water-Based Synthesis of Hybrid Silica/Hyperbranched Poly(ethylene imine) Nanopowder for Heavy Metal Sorption from Aqueous Solutions

Ioanna Kitsou and Athena Tsetsekou

School of Mining Engineering & Metallurgy, National Technical University of Athens, 9 Iroon Polytechniou, Zografou Campus, 15780 Athens, Greece

Correspondence should be addressed to Athena Tsetsekou; athtse@metal.ntua.gr

Received 20 July 2018; Accepted 23 October 2018; Published 9 January 2019

Academic Editor: Miguel A. Correa-Duarte

A novel hybrid, water-based, sol-gel method was developed for the synthesis of functionalized silica with advanced adsorptive capacities towards heavy metal ions. The study employs the hyperbranched poly(ethylene imine) (HBPEI) as a reactive template for the synthesis of silica. The reaction was followed by FTIR, whereas the material was evaluated in terms of its microstructure and adsorptive properties. The results revealed a very potent adsorbent that can remove heavy metal ions (namely, Pb, Cu, and Zn) from water in a fast and efficient way. Greater selectivity was observed for lead, whereas the maximum adsorption capacities calculated from the Langmuir model were 833.3, 502.5, and 193.4 mg/g for lead, copper, and zinc, respectively.

1. Introduction

Heavy metal pollution in water is an issue of great concern, constituting a severe threat for the human health and ecological systems. Copper, lead, zinc, cadmium, mercury, and nickel are considered the most dangerous elements and are included in the US Environmental Protection Agency's (EPA) list of priority pollutants. The reason is their high toxicity in combination with their growing discharge in the environment and bioaccumulation effects. In fact, heavy metals, in contrast to the more toxic organic compounds, are not degradable, being accumulated in the environment and eventually ending up in the humans through the food chain [1–3].

Various techniques have been developed for the removal of metal ions from wastewater such as reverse osmosis, nanofiltration [4], ion exchange [5], adsorption [6], precipitation [7], and coagulation [8]. Among them, adsorption is one of the most effective methods for the remediation of heavy metal pollution [9] as the process offers flexibility in both design and operation, providing also in most of the cases the advantages of a reusable effluent and of an economic regeneration procedure due to its reversible nature [10].

Several adsorbents have been proposed to remove heavy metal ions from wastewater, such as plenteous and inexpensive cellulose and its modified forms [11], multifarious agricultural waste material, and potentially low cost sorbent clays [12], iron oxides, and hydroxides [13, 14] as well as carbon nanotubes [15]. Recently, dendritic polymers containing amine groups have shown a high binding capacity for metal ions dissolved in water. The properties of these materials are related to the degree of branching and the number of amino groups. Among them, the hyperbranched poly(ethylene imine) (HBPEI) is a low cost polymer, well known for its high activity and therefore high functionalization potential [16, 17].

HBPEI consists of a spheroidal, asymmetric structure with a high branching degree (between 65 and 75%) and relatively narrow polydispersity. It is a cationic polymer

demonstrating the maximum density of positive charge when it is protonated in an aqueous solution. These properties make HBPEI useful for a number of industrial applications such as in the paper industry for the flocculation of negatively charged fibers or as additive in paper production printers, in drug delivery systems. Its chemical properties and especially its proved high efficiency in entrapping heavy metals render it also very promising for applications in wastewater treatment and metal ion removal [18–21]. For these reasons, it is often used to increase the adsorption capacity of an adsorbent by modifying its surface. Such an adsorbent is usually silica that is a low-cost ceramic with excellent thermal and mechanical stability, unique large surface area, and easily modified surface characteristics [22]. Due to these excellent qualifications, silica is very often the material of choice for the immobilization of poly(ethylene imine) (PEI) to develop a hybrid for the effective removal of heavy metals from water [23].

Silica-based adsorbents have been developed by various ways over the years. Porous structures have been synthesized by sol-gel mainly in the presence of anionic and neutral substances or by utilizing hyperbranched polyesters and dendritic polymers as precursors or pore-forming agents [24–26]. The design of hybrid nanostructured materials has also drawn immense attention recently as these materials offer great potential for applications in many industrial fields including adsorption processes [27]. In this context, the surfactant method has been employed to synthesize mesoporous silica materials with controlled porosity and structure by changing the type or length of the chain of the surfactant matrix. The as-synthesized silica powders were subsequently functionalized with organoalkoxysilanes and tested for their adsorptive capacity to remove heavy metals from drinking water. Hybrid organic-inorganic nanospheres synthesized through the interaction of HBPEI with silicic acid in water have also been used successfully for the sorption of toxic metal ions and polycyclic aromatic hydrocarbons from water [16]. Further, novel adsorbents resulting from the functionalization of chitosan–silica hybrids with EDTA (ethylenediaminetetraacetic acid) ligands were also synthesized and tested for their adsorptive capacities with respect to Cu(II), Ni(II), Cd(II), and Pb(II) [28].

In this work, a functionalized silica network, synthesized through a water-based sol-gel approach, is evaluated as a potential adsorbent of heavy metals (Pb, Cu, and Zn) from contaminated water demonstrating excellent results. The synthesis approach involves the reaction of HBPEI with 3-(triethoxysilyl)propyl isocyanate (TESPI) followed by the subsequent hydrolysis and cross-linking sol-gel reactions. The whole procedure is based on the method discussed in our previous work [26] which can afford nanostructured, dendritic-based networks which upon calcination lead to nanoporous silica with tailored pore structure and high surface area (~600 to 1100 m^2/g depending on the conditions employed). However, in the present work, the organic solvent for HBPEI (N,N-dimethylformamide or chloroform) is replaced by water with the aim to further simplify the procedure and reduce both the cost of the material and the environmental drawbacks.

2. Experimental

2.1. Materials and Methods. Hyperbranched poly(ethylene imine) (HBPEI) (Mn = 25,000) and 3-(triethoxysilyl)-propyl isocyanate (TESPI, 95%) were provided by Sigma-Aldrich. Lead(II) nitrate ($Pb(NO_3)_2$, ≥99.99%) was provided by Aldrich, and zinc nitrate hexahydrate ($Zn(NO_3)_2{\cdot}6H_2O$, ≥99%) and copper nitrate hemi(pentahydrate) ($Cu(NO_3)_2{\cdot}2.5H_2O$, ≥98%) were purchased by Sigma-Aldrich.

2.2. Synthesis of Hybrid Network. The organic-inorganic network was prepared via a novel hybrid sol-gel templating route (Figure 1) which has been described in detail in our previous work [26]. However, in this case, the solvent employed was water. In short, appropriate amount of poly(-ethylene imine) was dissolved in ultrapure water so that the HBPEI : water molar ratio with respect to the sum of primary and secondary amino groups of HBPEI reaches the value 1 : 8. The addition of HBPEI was made under continuous stirring and after dissolution; the resulting solution was allowed to stand for about 30 min. Afterward, to this solution, which was kept at 0°C, 3-(triethoxysilyl)propyl isocyanate (TESPI) was added dropwise, under continuous stirring, to reach molar ratio SiO_2/HBPEI = 0.16, 0.35, or 0.8 and the reaction mixture was held at this temperature for one more hour. Then, it was allowed to reach room temperature where it remained for several minutes, again under continuous stirring, so that interaction between the terminal amino groups of hyperbranched poly(ethylene imine) and the isocyanate group of silica's precursor takes place. Finally, the reaction product was left for curing at room temperature for 24 hours, in order to attain hydrolysis of triethoxy groups and silanol formation, and then, it was dried at 90°C for 100 h to complete the formation of the silica network.

2.3. Characterization Techniques. The presence of the hyperbranched poly(ethylene imine) in the silica particles and the formation of the siloxane bridges were established by FTIR spectroscopy employing a Nicolet Magna-IR 550 Spectrometer. Thermogravimetry experiments were also performed up to 1000°C under air flow at a heating rate of 10°C/min, employing a TGA 2050 analyzer (TA Instruments).

The morphology and the microstructure of dispersed powder were examined with a high-resolution transmission electron microscope (HRTEM, JEOL 2100 HR). Bright field images were recorded over selected areas for this purpose. The sample was washed several times with deionized water and acetone, in order to remove the excess of the polymer and to have a better observation of it. Portions of samples were crushed in an agate mortar and suspended in ethanol.

2.4. Heavy Metal Adsorption Experiments. For the investigation of the adsorption of heavy metals on nanohybrid surfaces, adsorption experiments were made by varying the concentration of metals into pure water as well as the contact time. For the realization of adsorption as a function of

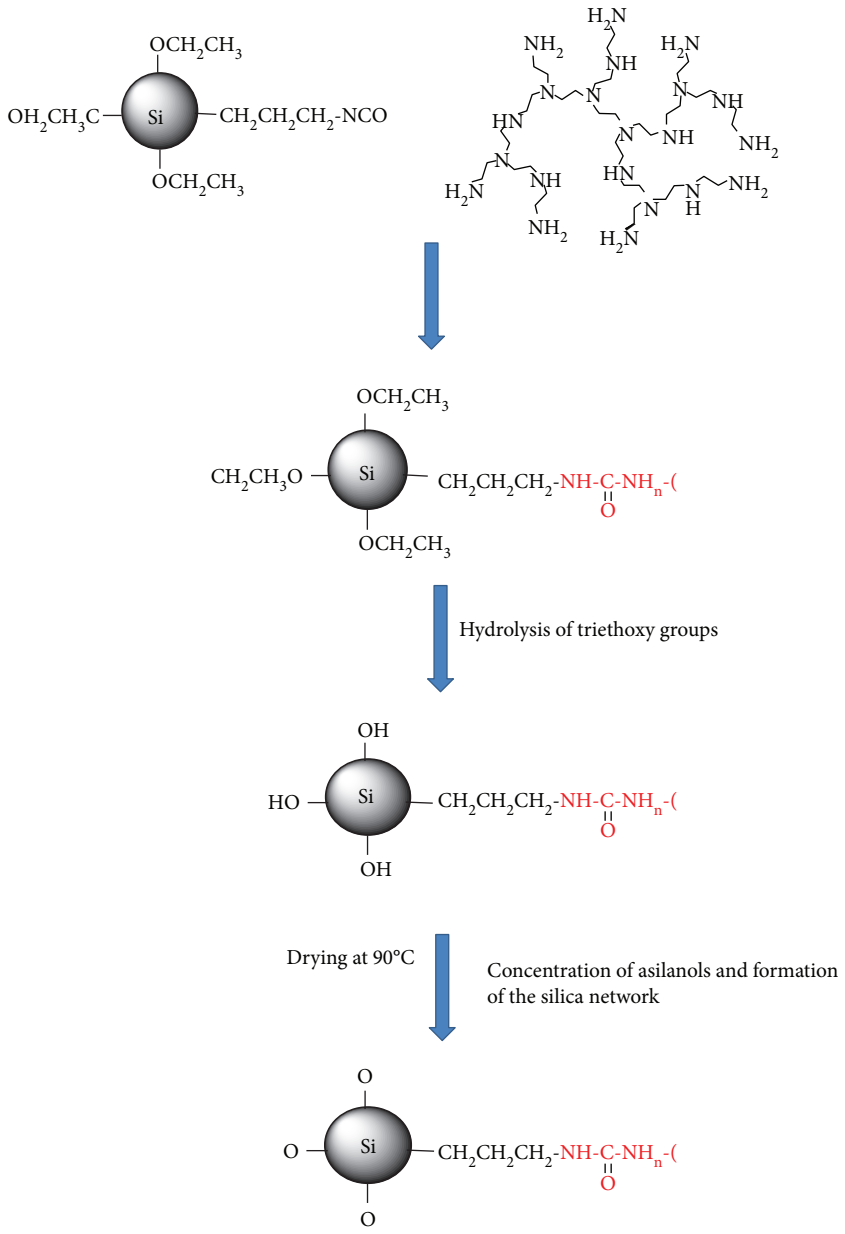

Figure 1: Schematic representation of the reaction for the hybrid material synthesis.

concentration of metals, 2.5 mg of the hybrid material (SiO_2-HBPEI-0.16) was dispersed in 10 mL ultrapure water. The pH value was adjusted with 0.1 M HCl and 0.1 M NaOH and kept at 6.2. Then, the appropriate volume of standard solution was added to a suspension of metal so that the final concentration of the metal is 200 ppm, 150 ppm, 100 ppm, 80 ppm, 60 ppm, 40 ppm, 20 ppm, and 10 ppm, and the suspension was allowed under stirring at room temperature for 24 hours in order to ensure that the adsorption equilibrium is reached. The pH values even after the adsorption process were remained at the range of 6.1–6.2. The concentration of the metal ions in the solution was measured using an atomic absorption spectrophotometer (AS-PerkinElmer 4100). The adsorption capacity of the adsorbent at equilibrium was calculated as follows:

$$Q_e = V\frac{C_0 - C_e}{m}, \quad (1)$$

where Q_e is the equilibrium adsorption capacity of the adsorbent in mg/g, C_0 is the initial concentration in mg/L, C_e is the concentration at equilibrium of metal ions in mg/L, V is the volume in L of metal ion solution, and m is the weight in g of the adsorbent [29].

The kinetics of the adsorption process was investigated to study the effect of the initial concentration of metal ions on q with respect to time and the time required to achieve

equilibrium between aqueous and solid phases. The kinetics study was carried out using 2.5 mg material dispersed in 10 mL of 1 ppm Pb(II), Cu(II), and Zn(II) metal ion solutions. The suspensions were left under stirring for 5 min, 10 min, 15 min, 30 min, 2 h, 6 h, 12 h, and 1 day. The concentration of the pollutant in the supernatant was determined spectrophotometrically as described above. The removal efficiency, R, of the heavy metal ions was calculated by the following equation:

$$R(\%) = \frac{C_0 - C_t}{C_0} * 100, \quad (2)$$

where C_0 is the initial concentration of the metal ions (mg/L) and C_t is the concentration of the metal ions (mg/L) at time t [30].

3. Results and Discussion

3.1. FTIR Analysis. FTIR analysis was employed to follow the reactions occurring for the formation of the hybrid silica network functionalized with HBPEI (Figure 2).

It is well known in literature the reaction of isocyanates with water. The kinetics of this reaction to form urea as a final product is studied in detail in the work of Hai et al. [31]. The isocyanate group reacts initially with water to form an intermediate, unstable, carbamic acid which spontaneously decarboxylates into a primary amine and carbon dioxide. The amine, in turn, reacts again with another isocyanate group producing a urea cross-link. Since, in our case, the reaction of TESPI with HBPEI was performed in water, we also examined by the FTIR characterization technique a sample that was developed following the same procedure but in the absence of HBPEI (named as SiO_2-free of HBPEI). The reason was to examine if HBPEI is finally involved in the formation of the silicate network, since, in this case, there coexists the reaction of TESPI with water. For this reason, materials received employing different TESPI to HBPEI molar ratios (see Experimental) were also analyzed by FTIR. The patterns of the different materials that were synthesized as well as the pattern received from the HBPEI itself are depicted and compared in Figure 2.

Examining the spectrum of the SiO_2 free of the HBPEI sample (the sample prepared in the absence of HBPEI during reaction), it becomes obvious that a different material has been produced compared to the one synthesized employing the highest amount (ratio of TESPI to HBPEI, 0.16) of HBPEI whereas the spectra of the other materials, with intermediate HBPEI content during reaction, present a progressive evolution from the pattern of the HBPEI-free sample to the one with the highest polymer content. In fact, in the spectrum of the SiO_2 free of HBPEI sample, strong bands are revealed, characteristic of the urea bonds' vibrations. These are the bands at 3335 cm^{-1}, 1695 cm^{-1}, 1630 cm^{-1}, 1479 cm^{-1}, and 1016 cm^{-1}, which are assigned to the N-H stretching, C=O stretching, N-H deformation, C-N asymmetric stretching, and C-N symmetric stretching vibrations in urea, respectively [32, 33]. Therefore, in agreement with the literature data, in the case of the HBPEI-free sample, the TESPI reacts with water leading to the formation of urea links.

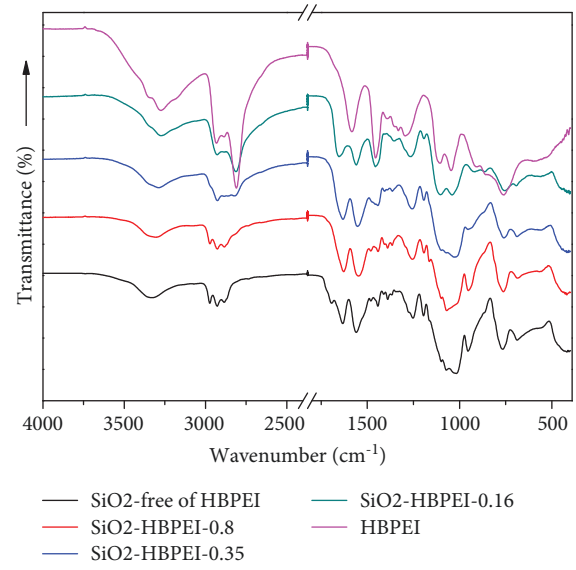

Figure 2: FTIR spectra of HBPEI, SiO_2-HBPEI-0.16, SiO_2-HBPEI-0.35, SiO_2-HBPEI-0.8, and SiO_2-free of HBPEI.

In contrast, all these characteristic urea bands are totally absent from the SiO_2-HBPEI-0.16 sample. This permits the hypothesis that in this sample the reactions followed a different path involving the HBPEI. The spectrum of this sample reveals the characteristic vibration of the amide I band vibration at 1654 cm^{-1} suggesting the formation of secondary amide groups possibly through the reaction of isocyanate groups of TESPI with the primary amino groups of HBPEI. The reaction of HBPEI amino groups with the precursor of silica (TESPI) is evidenced by the absence of the N–H asymmetric stretching vibration in HBPEI at 3350 cm^{-1}, while the symmetric stretching is hardly observed at 3276 cm^{-1} [26]. In addition, the absorption band attributed to the bending of the NH_2 groups in the HBPEI spectrum at 1583 cm^{-1} is absent from the spectrum of the SiO_2-HBPEI supporting the reaction of HBPEI [16].

Further, the absence of antisymmetric (2974 cm^{-1}) and symmetric (2885 cm^{-1}) stretching vibrations of the methyl groups from the spectrum of the SiO_2-HBPEI-0.16 sample suggests the hydrolysis of ethoxysilane groups to silanols. The weak band at 921 cm^{-1} corresponding to the stretching vibrations of the Si-OH groups further supports the assumption of hydrolysis of ethoxysilane groups [26]. Again, the SiO_2 free of the HBPEI sample shows a different spectrum regarding the hydrolysis degree, as it reveals the bands at 2975 cm^{-1} and 2883 cm^{-1} as well as a band at 953 cm^{-1} corresponding to the vibration zone of H_3C-C groups, whereas the band at 921 cm^{-1} is absent. Therefore, it can be derived that, in this case where the HBPEI is not present in the reaction, the hydrolysis of ethoxysilanes is incomplete [26].

The formation of the silica network as a result of the condensation of silanols to form Si-O-Si bonds in the SiO_2-HBPEI-0.16 sample can be evidenced by the presence in the spectrum of the characteristic vibrations at 1103 cm^{-1} and

at 1040 cm^{-1} assigned to the transverse optical stretching modes of Si-O-Si bonds which are present in large cyclic structures of the dense network of silica [34–36] and in smaller siloxane rings encountered in the sol [26], respectively. A band associated with Si-O rocking can be also observed at 455 cm^{-1} [35].

Finally, the hybrid nature of the silica network in the SiO_2-HBPEI-0.16 sample is evidenced by the presence of the asymmetric and symmetric stretching bands of CH_2 that appear at 2931 cm^{-1} and 2809 cm^{-1} [26]. Further, the bands at 1454 cm^{-1} and 1363 cm^{-1} correspond to asymmetric and symmetric vibrations of CH_2, respectively [36], while this at 753 cm^{-1} is assigned to the zone oscillation of CH_2 [16].

3.2. XRD Analysis. To confirm the formation of the silica network, the SiO_2-HBPEI-0.16 material (prepared with the highest HBPEI content during synthesis) was analyzed by XRD in the as-received state and after calcination at different temperatures in the range 1000 to 1400°C. The as-received material is amorphous showing peaks which correspond to the polymer that is present in the structure. Upon calcination, these peaks disappear and the pattern corresponds to pure amorphous silica that is crystallized to cristobalite after calcination at 1400°C (Figure 3).

3.3. Thermogravimetric Analysis. Thermogravimetry analysis (TGA) of the SiO_2-HBPEI-0.16 material was performed under flowing air, up to 1000°C to investigate the presence of organic matter into the material. As it can be seen in Figure 4, a large mass loss reaching ~35% of the initial weight is revealed in the temperature range 100–800°C. The initial weight loss up to about 150°C, which is estimated at around 10%, can be attributed to the evaporation of moisture. However, further weight losses taking place at higher temperatures can be associated with the decomposition and burning of the hyperbranched polymer (an exothermal peak appears in the DTA curve at 350°C revealing the burning of polymer), with the dissociation of structural water and possibly with additional condensation reactions of silanol groups. These entire phenomena stop above 800°C as no further mass loss can be noticed, suggesting that up to this temperature HBPEI and amines have been fully decomposed affording silica free of any organic material.

3.4. TEM Analysis. A characteristic TEM image of the SiO_2-HBPEI-0.16 material is shown in Figure 5. As it can be seen, the material is consisted of particles with an almost spherical shape with diameters ranging between 3 and 10 nm.

3.5. Adsorption Isotherms for Heavy Metals. Finally, the material that was prepared with the highest HBPEI content during synthesis, namely, the SiO_2-HBPEI-0.16 material, was selected to be further evaluated for its adsorptive capacities towards heavy metals (Pb^{2+}, Cu^{2+}, and Zn^{2+}). For this, sorption experiments were performed by varying the contact time and the initial concentration of the metal ion into the water solution. The sorption isotherms received are depicted in Figure 6.

The material shows similar behavior in all three cases under investigation. Load increases with increasing concentration of the metal in the solution. However, there is different selectivity for each metal following the order Pb > Cu > Zn. In fact the maximum adsorption load measured in these experiments was 605.4, 462.2, and 188 mg/g for Pb(II), Cu (II), and Zn (II), respectively.

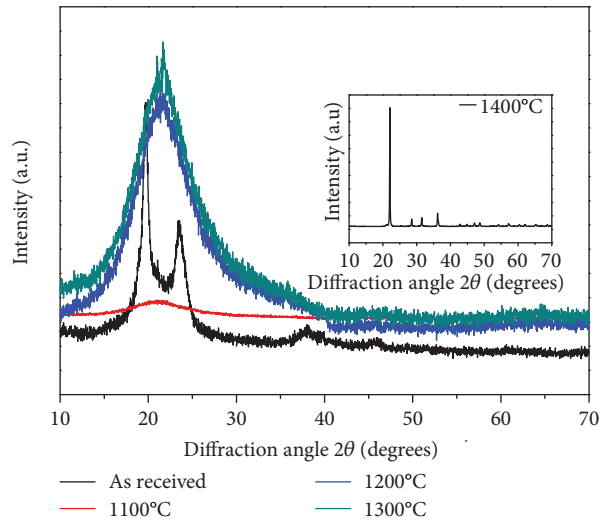

FIGURE 3: XRD patterns of SiO_2-HBPEI-0.16 as received and calcined at various temperatures.

Heavy metal sorption capacity of silica has been correlated to the cation ionic radius as metals of larger radius possess greater tendency to polarize and thus to form complexes with the deprotonated negatively charged silanol groups of silica surface. Similarly, the interaction strength between the metal ions and the amino groups in the hybrid material is also proportional to the metal ion polarization [37]. As a consequence, a greater bonding strength with both the amino and the silanol groups is expected for Pb^{2+} which exhibits the highest molecular weight and the largest electronegativity among the three ions (Pb(II), Zn(II), and Cu(II)) investigated [38], a fact that can explain the higher selectivity shown for Pb sorption.

Table 1 compares the results of the adsorption capacity for the adsorbent prepared in the present work to those obtained by various adsorbents reported by other authors [16, 23, 39–43]. It can be easily seen that the as-synthesized novel material is a very effective adsorbent of metal ions showing capacities much higher than the previously reported values.

The obtained experimental results were analyzed by the Langmuir adsorption model, which is based on the hypothesis that the maximum adsorption corresponds to a saturated monolayer of adsorbate molecules on the adsorbent surface. Consequently, adsorption appears uniformly on the adsorbent's active sites, and once an adsorbate occupies a site, no further adsorption will take place at this site. The Langmuir model is expressed by the following:

$$\frac{C_e}{Q_e} = \frac{C_e}{Q_{max}} + \frac{1}{bQ_{max}}, \quad (3)$$

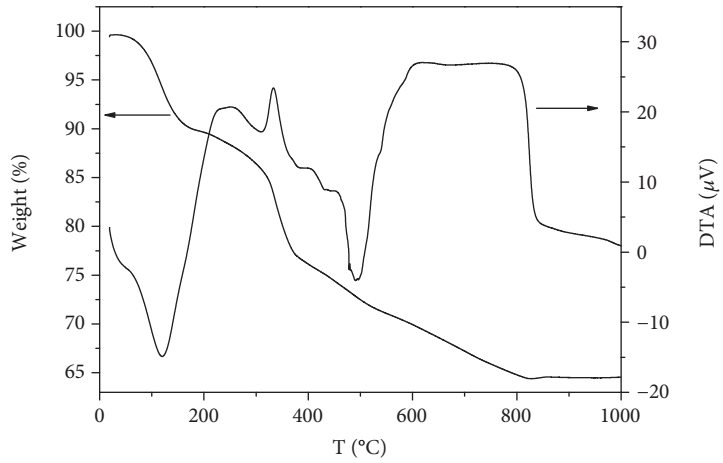

Figure 4: TGA pattern of the as-prepared nanopowder.

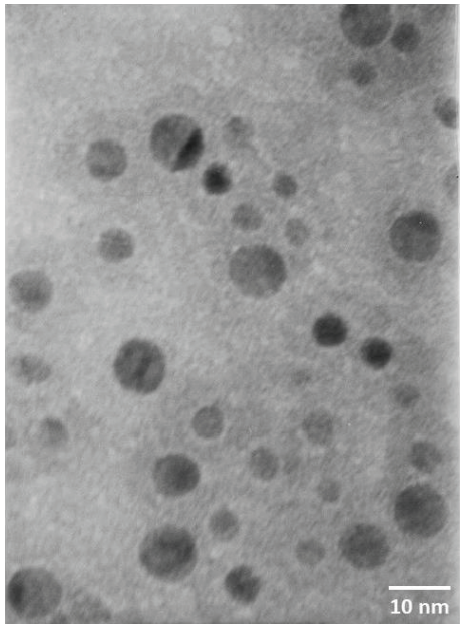

Figure 5: TEM image of the as-prepared nanoparticles.

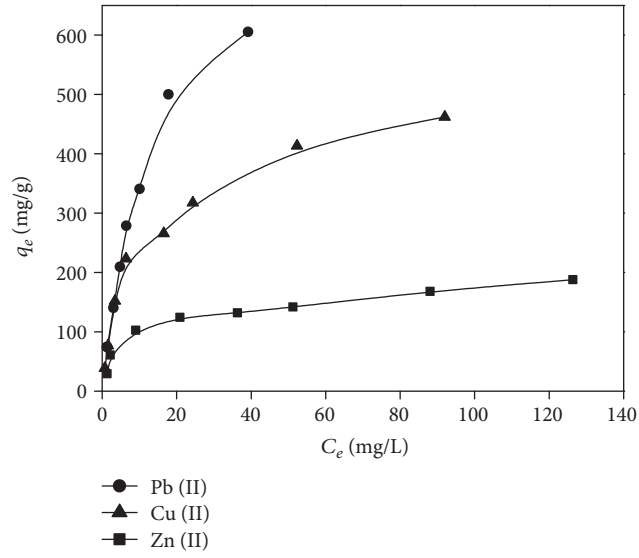

Figure 6: Sorption isotherms of Pb^{2+}, Cu^{2+}, and Zn^{2+} by SiO_2-HBPEI-0.16 (pH 6.2, contact time 24 h).

where Q_e is the equilibrium adsorption capacity of the adsorbent in mg/g, C_e is the concentration of residual solute in mg/L at equilibrium, Q_{max} is the maximum uptake of the adsorbent (mg/g), and b (L/mg) is the Langmuir constant that expresses the binding energy of adsorption (affinity) [44].

Therefore, with the proper processing of experimental results by Langmuir equation (3), the related constant value b and the value Q_{max} were calculated (Figure 7). These values along with the nonlinear regression correlation coefficients (R^2) for Langmuir isotherms are given in Table 2.

As it can be seen in Table 2, the correlation coefficients (R^2) were very high in all three cases examined, suggesting that the adsorption follows the Langmuir model. Further, the analysis of the results confirmed that the SiO_2/HBPEI hybrid nanopowder exhibits very high adsorption capacities following the order Pb(II) > Cu(II) > Zn(II) in accordance with the experimental results discussed above.

The type of the Langmuir isotherm can be also used to predict whether the adsorption is favorable or unfavorable. This can be realized by either evaluating the equilibrium parameter (b) or a dimensionless constant separation factor R_L expressed as follows:

$$R_L = \frac{1}{1 + bC_0}, \tag{4}$$

where C_0 (mg/L) is the initial concentration of metal ion. In fact, for values of the separation factor constant $R_L < 1$, the adsorption is considered favorable, whereas the adsorption is considered unfavorable for $R_L > 1$ [45]. In this respect, the R_L values were calculated from the experimental data and their range for each system is also given in Table 2.

Table 1: Comparison of the maximum adsorption capacity of the as-synthesized SiO_2/HBPEI-0.16 material to the capacities of other adsorbents referred in literature.

Adsorbent	Adsorption capacity Q_{max} (mg/g)			Reference
	Pb(II)	Cu(II)	Zn(II)	
Organic/inorganic hybrid silica nanospheres	632.9	—	—	[16]
PEI-modified biomass	204	92	—	[23]
Xanthate-modified magnetic chitosan (XMCS)	76.9	34	20.8	[39]
Fe_3O_4 magnetic nanoparticles	166.1	126.9	43.4	[40]
Municipal solid mixed with green waste (MSGW)	196	36	24	[42]
Modified Pseudomonas Lk9-2P	480	210.2	—	[43]
Twice-mercerized sugarcane bagasse (MMSCB 2)	500	185.2	—	[44]
Hybrid SiO_2/HBPEI-0.16	833.3	502.5	193.4	Present work

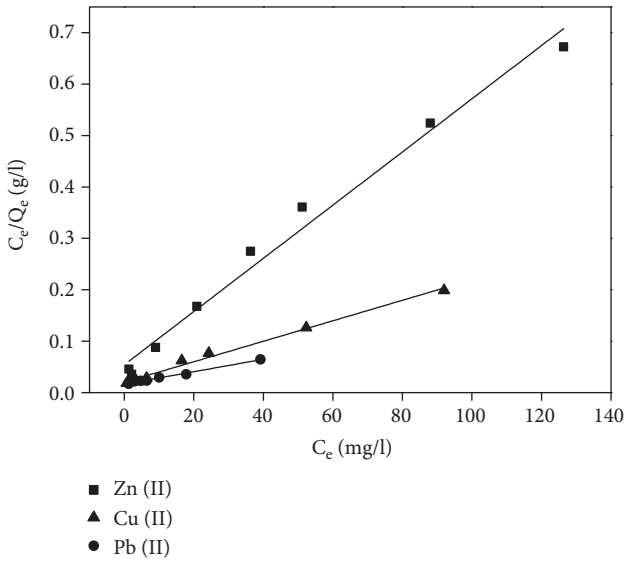

Figure 7: Sorption isotherms by Langmuir.

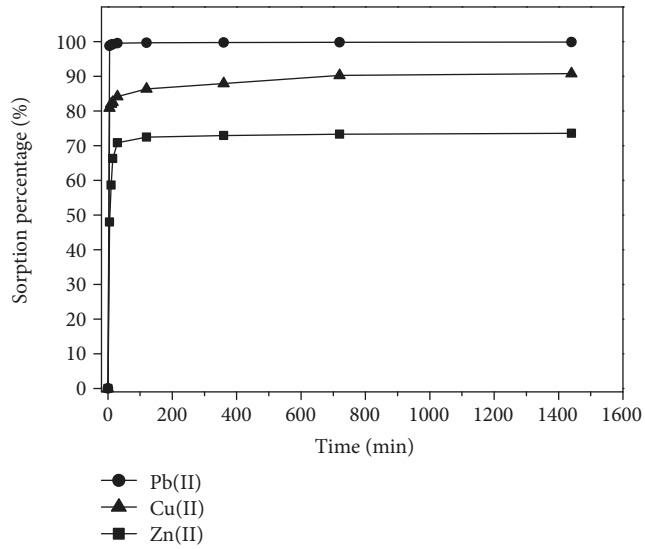

Figure 8: Sorption kinetics of Pb^{2+}, Cu^{2+}, and Zn^{2+} by SiO_2-HBPEI-0.16 (C_o = 1 ppm, pH = 6.2).

Table 2: Sorption parameters for the Langmuir model.

Isotherm parameters	Pb	Cu	Zn
Q_{max} (mg/g)	833.3	502.5	193.4
b (L/mg)	0.073	0.098	0.095
R^2	0.9915	0.9908	0.9829
R_L range	0.063–0.577	0.048–0.503	0.344–0.910

The results show values smaller than unity suggesting a favorable adsorption in all cases.

3.6. Adsorption Kinetics. The results of kinetic experiments are presented in Figure 8. The loading of all three metal ions on the material increases rapidly in the first five minutes followed by a very slow increase up to one day. In complete agreement with the data obtained from the analysis of the adsorption isotherms, the greatest load during the period of the first five minutes is measured for lead, confirming the strong chelating ability of the hybrid SiO_2-HBPEI-0.16 material to Pb^{2+} [16].

Adsorption kinetic parameters, i.e., the rate constants and equilibrium adsorption capacities, which can provide valuable insights into wastewater treatment process design, are of great importance for the application of adsorbents. In order to evaluate the kinetic adsorption mechanism, the pseudo-first-order (5) and pseudo-second-order (6) models were investigated:

$$\ln\left(q_{e,cal} - q_t\right) = \ln q_{e,cal} - k_1 t, \tag{5}$$

$$\frac{t}{q_t} = \frac{1}{k_2 q_{e,cal}^2} + \frac{1}{q_{e,cal}} t, \tag{6}$$

where $q_{e,cal}$ is the amount of metal adsorbed at equilibrium (mg g^{-1}), q_t is the amount of metal ions adsorbed at time t (mg g^{-1}), and k_1 and k_2 are the rate constants of pseudo-first-order and pseudo-second-order (g mg^{-1} min^{-1}) models, respectively [46].

The calculated parameters of the two models are summarized in Table 3. Based on the correlation coefficients R^2, the

Table 3: Parameters of the pseudo-first-order and pseudo-second-order models of Pb(II), Cu(II), and Zn(II) onto silica nanopowder.

	Pb	Cu	Zn
Pseudo-first-order model			
k_1 (min^{-1})	$1.13 * 10^{-3}$	$4.889 * 10^{-4}$	$-2.664 * 10^{-4}$
$q_{e,cal}$ (mg/g)	4.05	0.45	0.19
R^2	0.626	0.756	0.182
Pseudo-second-order model			
k_2 ($g\,mg^{-1}\,min^{-1}$)	1.776	0.076	0.153
$q_{e,cal}$ (mg/g)	3.58	3.51	2.55
R^2	1	0.999	1
$q_{e,exp}$ (mg/g)	3.58	3.51	2.55

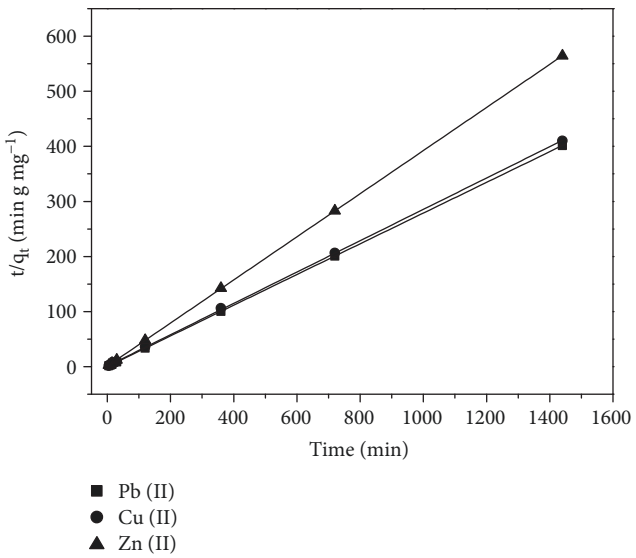

Figure 9: Pseudo-second-order sorption kinetics of Pb^{2+}, Cu^{2+}, and Zn^{2+} onto SiO_2-HBPEI-0.16.

results clearly indicate that the adsorption kinetics follow the pseudo-second-order kinetic model (Figure 9). Furthermore, the equilibrium adsorption capacities calculated ($q_{e,cal}$) based on the pseudo-second-order model are in perfect agreement with the experimental data ($q_{e,exp}$). The fitting of this model suggests that chemisorption is the controlling mechanism with the sorption capacity being proportional to the number of active sites on the hybrid silica [47].

4. Conclusions

In this research, an environmentally friendly method for the preparation of hybrid materials with improved adsorptive properties was developed and implemented. The synthesis concerns a cost effective process, performed in water, which employs hyperbranched PEI as a reactive template for the synthesis and simultaneous functionalization of silica nanopowder.

The results of FTIR confirmed that the proposed synthesis method is effective leading to the successful substitution of the amino groups of the silane and the successful formation of the silica network. The hybrid material has a spherical shape with a mean diameter at about 7 nm.

The as-synthesized hybrid (SiO_2-HBPEI-0.16) material was evaluated for its adsorption potential to remove heavy metal ions (namely, Zn^{2+}, Pb^{2+}, and Cu^{2+}) from water. The adsorption experiments demonstrated that the material is an excellent adsorbent. Greater selectivity was shown for lead followed by that for copper. The kinetics experiments revealed that the process of adsorption is carried out in a relatively short time (5 min) as the metal loading on the material increases strongly during this time.

Data Availability

The data used to support the findings of this study are available from the corresponding author upon request.

Conflicts of Interest

The authors declare that there is no conflict of interest regarding the publication of this paper.

References

[1] G. Grigoropoulou, P. Stathi, M. A. Karakassides, M. Louloudi, and Y. Deligiannakis, "Functionalized SiO_2 with N-, S-containing ligands for Pb(II) and Cd(II) adsorption," *Colloids and Surfaces A: Physicochemical and Engineering Aspects*, vol. 320, no. 1-3, pp. 25–35, 2008.

[2] B. Gao, Y. Gao, and Y. Li, "Preparation and chelation adsorption property of composite chelating material poly(amidoxime)/SiO_2 towards heavy metal ions," *Chemical Engineering Journal*, vol. 158, no. 3, pp. 542–549, 2010.

[3] E. Y. Jeong, M. B. Ansari, Y. H. Mo, and S. E. Park, "Removal of Cu(II) from water by tetrakis (4-carboxyphenyl) porphyrin-functionalized mesoporous silica," *Journal of Hazardous Materials*, vol. 185, no. 2-3, pp. 1311–1317, 2011.

[4] H. A. Qdais and H. Moussa, "Removal of heavy metals from wastewater by membrane processes: a comparative study," *Desalination*, vol. 164, no. 2, pp. 105–110, 2004.

[5] R. N. Ntimbani, G. S. Simate, and S. Ndlovu, "Removal of copper ions from dilute synthetic solution using staple ion exchange fibres: equilibrium and kinetic studies," *Journal of Environmental Chemical Engineering*, vol. 3, no. 2, pp. 1258–1266, 2015.

[6] J. Ma, G. Qin, Y. Zhang, J. Sun, S. Wang, and L. Jiang, "Heavy metal removal from aqueous solutions by calcium silicate powder from waste coal fly-ash," *Journal of Cleaner Production*, vol. 182, pp. 776–782, 2018.

[7] R. R. Navarro, S. Wada, and K. Tatsumi, "Heavy metal precipitation by polycation–polyanion complex of PEI and its phosphonomethylated derivative," *Journal of Hazardous Materials*, vol. 123, no. 1-3, pp. 203–209, 2005.

[8] A. G. El Samrani, B. S. Lartiges, and F. Villiéras, "Chemical coagulation of combined sewer overflow: heavy metal removal and treatment optimization," *Water Research*, vol. 42, no. 4-5, pp. 951–960, 2008.

[9] R. K. Gautam, M. C. Chattopadhyaya, S. K. Sharma, S. K. Sharma, and R. Sanghi, Eds., *Biosorption of Heavy Metals: Recent Trends and Challenges*, E-Publishing Inc., New York, 2013.

[10] Y. Pang, G. Zeng, L. Tang et al., "PEI-grafted magnetic porous powder for highly effective adsorption of heavy metal ions," *Desalination*, vol. 281, pp. 278–284, 2011.

[11] S. Li, W. Wang, F. Liang, and W.-x. Zhang, "Heavy metal removal using nanoscale zero-valent iron (nZVI): theory and application," *Journal of Hazardous Materials*, vol. 322, Part A, pp. 163–171, 2017.

[12] Y. Zhang, L. Xu, L. Zhao et al., "Radiation synthesis and Cr(VI) removal of cellulose microsphere adsorbent," *Carbohydrate Polymers*, vol. 88, no. 3, pp. 931–938, 2012.

[13] A. Demirbas, "Heavy metal adsorption onto agro-based waste materials: a review," *Journal of Hazardous Materials*, vol. 157, no. 2-3, pp. 220–229, 2008.

[14] A. García-Sánchez, A. Alastuey, and X. Querol, "Heavy metal adsorption by different minerals: application to the remediation of polluted soils," *Science of The Total Environment*, vol. 242, no. 1-3, pp. 179–188, 1999.

[15] M. A. Tofighy and T. Mohammadi, "Adsorption of divalent heavy metal ions from water using carbon nanotube sheets," *Journal of Hazardous Materials*, vol. 185, no. 1, pp. 140–147, 2011.

[16] M. Arkas and D. Tsiourvas, "Organic/inorganic hybrid nanospheres based on hyperbranched poly(ethylene imine) encapsulated into silica for the sorption of toxic metal ions and polycyclic aromatic hydrocarbons from water," *Journal of Hazardous Materials*, vol. 170, no. 1, pp. 35–42, 2009.

[17] I. Kitsou, E. Roussi, and A. Tsetsekou, "Synthesis of aqueous nanodispersed nanocrysralline ceria suspensions by a novel organic/inorganic precipitation method," *Ceramics International*, vol. 43, no. 4, pp. 3861–3865, 2017.

[18] J. Liu and X. Wang, "Novel silica-based hybrid adsorbents: lead(II) adsorption isotherms," *The Scientific World Journal*, vol. 2013, Article ID 897159, 6 pages, 2013.

[19] L. Zhang, C. H. Hu, S. X. Cheng, and R. X. Zhuo, "PEI grafted hyperbranched polymers with polyglycerol as a core for gene delivery," *Colloids and Surfaces B: Biointerfaces*, vol. 76, no. 2, pp. 427–433, 2010.

[20] A. Von Harpe, H. Petersen, Y. Li, and T. Kissel, "Characterization of commercially available and synthesized polyethylenimines for gene delivery," *Journal of Controlled Release*, vol. 69, no. 2, pp. 309–322, 2000.

[21] M. Krämer, J.-F. Stumbé, G. Grimm et al., "Dendritic polyamines: simple access to new materials with defined treelike structures for application in nonviral gene delivery," *Chembiochem*, vol. 5, no. 8, pp. 1081–1087, 2004.

[22] P. Yin, Q. Xu, R. Qu, G. Zhao, and Y. Sun, "Adsorption of transition metal ions from aqueous solutions onto a novel silica gel matrix inorganic–organic composite material," *Journal of Hazardous Materials*, vol. 173, no. 1-3, pp. 710–716, 2010.

[23] S. Deng and Y. P. Ting, "Characterization of PEI-modified biomass and biosorption of Cu(II), Pb(II) and Ni(II)," *Water Research*, vol. 39, no. 10, pp. 2167–2177, 2005.

[24] S. Volden, W. R. Glomm, H. Magnusson, G. Øye, and J. Sjöblom, "Dendrimers and hyperbranched polyesters as structure-directing agents in the formation of nanoporous silica," *Journal of Dispersion Science and Technology*, vol. 27, no. 6, pp. 893–897, 2006.

[25] E. Pabón, J. Retuert, and R. Quijada, "Synthesis of mixed silica–titania by the sol–gel method using polyethylenimine: porosity and catalytic properties," *Journal of Porous Materials*, vol. 14, no. 2, pp. 151–158, 2007.

[26] D. Tsiourvas, A. Tsetsekou, A. Papavasiliou, M. Arkas, and N. Boukos, "A novel hybrid sol-gel method for the synthesis of highly porous silica employing hyperbranched poly(ethyleneimine) as a reactive template," *Microporous and Mesoporous Materials*, vol. 175, pp. 59–66, 2013.

[27] K. Xia, R. Z. Ferguson, M. Losier, N. Tchoukanova, R. Brüning, and Y. Djaoued, "Synthesis of hybrid silica materials with tunable pore structures and morphology and their application for heavy metal removal from drinking water," *Journal of Hazardous Materials*, vol. 183, no. 1-3, pp. 554–564, 2010.

[28] E. Repo, J. K. Warchoł, A. Bhatnagar, and M. Sillanpaa, "Heavy metals adsorption by novel EDTA-modified chitosan–silica hybrid materials," *Journal of Colloid and Interface Science*, vol. 358, no. 1, pp. 261–267, 2011.

[29] B. Gao, F. An, and K. Liu, "Studies on chelating adsorption properties of novel composite material polyethyleneimine/-silica gel for heavy-metal ions," *Applied Surface Science*, vol. 253, no. 4, pp. 1946–1952, 2006.

[30] M. Min, L. Shen, G. Hong et al., "Micro-nano structure poly(ether sulfones)/poly(ethyleneimine) nanofibrous affinity membranes for adsorption of anionic dyes and heavy metal ions in aqueous solution," *Chemical Engineering Journal*, vol. 197, pp. 88–100, 2012.

[31] H. Ni, H. A. Nash, J. G. Worden, and M. D. Soucek, "Effect of catalysts on the reaction of an aliphatic isocyanate and water," *Journal of Polymer Science Part A: Polymer Chemistry*, vol. 40, no. 11, pp. 1677–1688, 2002.

[32] Z. Plasek and T. Urbanski, "The infra-red absorption spectrum and structure of urea," *Bulletin E\E L'Academie Polonaise Des Sciences, Serle Des Sciences Chimiques*, vol. X, no. 3, 1962.

[33] D. Castro-Enríquez, F. Rodríguez-Félix, B. Ramírez-Wong et al., "Preparation, characterization and release of urea from wheat gluten electrospun membranes," *Materials*, vol. 5, no. 12, pp. 2903–2916, 2012.

[34] J. Wang, S. Fan, W. Zhao, and H. Zhang, "Assembly and luminescence properties of lanthanide-polyoxometalates/polyethyleneimine/SiO_2 particles with core–shell structure," *Thin Solid Films*, vol. 527, pp. 170–174, 2013.

[35] B. Arkles, *Infrared Analysis of Organosilicon Compounds: Spectra-Structure Correlations, Reprinted from Silicon Compounds: Silanes & Silicones*, Gelest, Inc, Morrisville, PA, USA, 2013.

[36] Z. Sassi, J. C. Bureau, and A. Bakkali, "Structural characterization of the organic/inorganic networks in the hybrid material (TMOS-TMSM-MMA)," *Vibrational Spectroscopy*, vol. 28, no. 2, pp. 251–262, 2002.

[37] S. Hao, Y. Zhong, F. Pepe, and W. Zhu, "Adsorption of Pb^{2+} and Cu^{2+} on anionic surfactant-templated amino-functionalized mesoporous silicas," *Chemical Engineering Journal*, vol. 189-190, pp. 160–167, 2012.

[38] A. Shahbazi, H. Younesi, and A. Badiei, "Functionalized SBA-15 mesoporous silica by melamine-based dendrimer amines for adsorptive characteristics of Pb(II), Cu(II) and Cd(II) heavy metal ions in batch and fixed bed column," *Chemical Engineering Journal*, vol. 168, no. 2, pp. 505–518, 2011.

[39] Y. Zhu, J. Hu, and J. Wang, "Competitive adsorption of Pb(II), Cu(II) and Zn(II) onto xanthate-modified magnetic chitosan,"

Journal of Hazardous Materials, vol. 221-222, pp. 155–161, 2012.

[40] F. Ge, M. M. Li, H. Ye, and B. X. Zhao, "Effective removal of heavy metal ions Cd^{2+}, Zn^{2+}, Pb^{2+}, Cu^{2+} from aqueous solution by polymer-modified magnetic nanoparticles," *Journal of Hazardous Materials*, vol. 211-212, pp. 366–372, 2012.

[41] R. Paradelo and M. T. Barral, "Evaluation of the potential capacity as biosorbents of two MSW composts with different Cu, Pb and Zn concentrations," *Bioresource Technology*, vol. 104, pp. 810–813, 2012.

[42] S. Luo, X. Li, L. Chen, J. Chen, Y. Wan, and C. Liu, "Layer-by-layer strategy for adsorption capacity fattening of endophytic bacterial biomass for highly effective removal of heavy metals," *Chemical Engineering Journal*, vol. 239, pp. 312–321, 2014.

[43] L. V. A. Gurgel, R. P. d. Freitas, and L. F. Gil, "Adsorption of Cu(II), Cd(II), and Pb(II) from aqueous single metal solutions by sugarcane bagasse and mercerized sugarcane bagasse chemically modified with succinic anhydride," *Carbohydrate Polymers*, vol. 74, no. 4, pp. 922–929, 2008.

[44] W. Yang, P. Ding, L. Zhou, J. Yu, X. Chen, and F. Jiao, "Preparation of diamine modified mesoporous silica on multi-walled carbon nanotubes for the adsorption of heavy metals in aqueous solution," *Applied Surface Science*, vol. 282, pp. 38–45, 2013.

[45] J. Zhang, S. Zhai, S. Li et al., "Pb(II) removal of Fe_3O_4@SiO_2–NH_2 core–shell nanomaterials prepared via a controllable sol–gel process," *Chemical Engineering Journal*, vol. 215-216, pp. 461–471, 2013.

[46] J. Kong, Q. Yue, S. Sun et al., "Adsorption of Pb(II) from aqueous solution using keratin waste–hide waste: equilibrium, kinetic and thermodynamic modeling studies," *Chemical Engineering Journal*, vol. 241, pp. 393–400, 2014.

[47] W. Liu, J. Zhang, C. Cheng, G. Tian, and C. Zhang, "Ultrasonic-assisted sodium hypochlorite oxidation of activated carbons for enhanced removal of Co(II) from aqueous solutions," *Chemical Engineering Journal*, vol. 175, pp. 24–32, 2011.